Detailed α-decay study of ^{180}Tl

B. Andel,[1,*] A. N. Andreyev,[2,3,4] S. Antalic,[1] A. Barzakh,[5] N. Bree,[6] T. E. Cocolios,[6,4] V. F. Comas,[7] J. Diriken,[6] J. Elseviers,[6] D. V. Fedorov,[5] V. N. Fedosseev,[8] S. Franchoo,[9] L. Ghys,[6,10] J. A. Heredia,[7] M. Huyse,[6] O. Ivanov,[6] U. Köster,[11] V. Liberati,[12] B. A. Marsh,[8] K. Nishio,[3] R. D. Page,[13] N. Patronis,[6,14] M. D. Seliverstov,[6,4] I. Tsekhanovich,[15,16] P. Van den Bergh,[6] J. Van De Walle,[4] P. Van Duppen,[6] M. Venhart,[17] S. Vermote,[18] M. Veselský,[17] and C. Wagemans[18]

[1]*Department of Nuclear Physics and Biophysics, Comenius University in Bratislava, 84248 Bratislava, Slovakia*
[2]*Department of Physics, University of York, York YO10 5DD, United Kingdom*
[3]*Advanced Science Research Center, Japan Atomic Energy Agency, Tokai-mura, Ibaraki 319-1195, Japan*
[4]*ISOLDE, CERN, CH-1211 Geneve 23, Switzerland*
[5]*Petersburg Nuclear Physics Institute, NRC Kurchatov Institute, 188300 Gatchina, Russia*
[6]*KU Leuven, Instituut voor Kern- en Stralingsfysica, University of Leuven, B-3001 Leuven, Belgium*
[7]*GSI-Helmholtzzentrum für Schwerionenforschung GmbH, 64291 Darmstadt, Germany*
[8]*EN Department, CERN, CH-1211 Geneve 23, Switzerland*
[9]*Institut de Physique Nucléaire, IN2P3-CNRS/Université Paris-Sud, F-91406 Orsay Cedex, France*
[10]*Belgian Nuclear Research Center SCK•CEN, Boeretang 200, B-2400 Mol, Belgium*
[11]*Institut Laue Langevin, 6 rue Jules Horowitz, F-38042 Grenoble Cedex 9, France*
[12]*School of Engineering and Science, University of the West of Scotland, Paisley PA1 2BE, United Kingdom*
[13]*Department of Physics, Oliver Lodge Laboratory, University of Liverpool, Liverpool L69 7ZE, United Kingdom*
[14]*Department of Physics, University of Ioannina, GR-45110 Ioannina, Greece*
[15]*School of Physics and Astronomy, University of Manchester, Manchester M13 9PL, United Kingdom*
[16]*Centre d'Etudes Nucleaires de Bordeaux Gradignan, F-33175 Gradignan Cedex, France*
[17]*Institute of Physics, Slovak Academy of Sciences, 84511 Bratislava, Slovakia*
[18]*Department of Physics and Astronomy, University of Gent, Proeftuinstraat 86, B-9000 Gent, Belgium*

(Received 15 August 2017; published 28 November 2017)

A detailed α-decay spectroscopy study of ^{180}Tl has been performed at ISOLDE (CERN). Z-selective ionization by the Resonance Ionization Laser Ion Source (RILIS) coupled to mass separation provided a high-purity beam of ^{180}Tl. Fine-structure α decays to excited levels in the daughter ^{176}Au were identified and an α-decay scheme of ^{180}Tl was constructed based on an analysis of α-γ and α-γ-γ coincidences. Multipolarities of several γ-ray transitions deexciting levels in ^{176}Au were determined. Based on the analysis of reduced α-decay widths, it was found that all α decays are hindered, which signifies a change of configuration between the parent and all daughter states.

DOI: 10.1103/PhysRevC.96.054327

I. INTRODUCTION

Odd-odd nuclei in the $Z = 82$ region are well known for a complex pattern of closely spaced multiplet states at low excitation energy arising from coupling of the odd proton with the odd neutron (see, e.g., [1–3] and references therein). The relative position of the states within the multiplet may depend on the neutron number; see the discussion in [4]. As α decay is very sensitive to changes of spin, parity, or configuration between initial and final states, α-decay spectroscopy is a valuable technique for investigating complicated level schemes [5]. The method is especially effective for identification of low-lying excited levels in daughter nuclei when α-γ coincidences are also measured. Evaluation of reduced α-decay widths (hindrance) for specific α-decay transitions and determination of γ-ray multipolarities can provide information on the configuration of the nuclear states involved.

This study of ^{180}Tl continues our systematic work on the series of odd-odd Tl isotopes investigated at ISOLDE: ^{178}Tl [6], ^{180}Tl [7–9], ^{182,184}Tl [5,10,11]. A common feature in all these studies was a persistent hindrance for all observed α decays between the parent and daughter nuclei, which signifies their different configurations; see the detailed discussion in the above-mentioned references.

Previous α-decay studies of ^{180}Tl were performed at the Argonne Tandem Linac Accelerator System (ATLAS) facility at Argonne National Laboratory in two experiments [12,13]. In both cases, fusion-evaporation reactions were employed and products separated by the Fragment Mass Analyzer (FMA) were implanted into a double-sided silicon strip detector. Statistics collected in each experiment were of the order of several hundred counts. Deduced α-decay energies are listed in Table I. In the second experiment, α-γ coincidences were also measured.

In our study, we registered $\approx 8 \times 10^5$ α decays of ^{180}Tl, which, in combination with α-γ coincidence analysis, allowed us to identify many weak fine-structure decays to excited states

*boris.andel@fmph.uniba.sk

TABLE I. α-decay properties of ^{180}Tl deduced in this work, in comparison with the previous studies. α-decay energies (E_α), coincident γ-ray transitions (E_γ), $Q_{\alpha,\mathrm{tot}}$ values, relative intensities of α-decay transitions (I_α), and their reduced decay widths (δ_α^2) are listed. Relative intensities were determined from α-γ coincidences[a] (except for the 6553-keV decay). Single-step γ-ray transitions directly deexciting levels in ^{176}Au and thus defining their energies are in bold. Coincidences shown in italics are tentative.

Ref. [12] $T_{1/2} = 1.5(2)$ s		Ref. [13] $T_{1/2} = 1.1(2)$ s		This work $T_{1/2} = 1.09(1)$ s[b]				
E_α (keV)	I_α (%)	E_α (keV)	E_γ (keV)	E_α (keV)	E_γ[c] (keV)	$Q_{\alpha,\mathrm{tot}}$ (keV)	I_α[a] (%)	δ_α^2 (keV)
6560(10)	15(3)	6558(10)		6553(7)		6702(7)	12.9(5)	0.16(11)
6470(20)[d]	7(3)	6490(10)[d]						
6362(10)	30(6)	6367(10)	**204.8(5)**	6354(7)	**204.8**	6704(7)	39.8(36)	2.9(19)
				6348(7)	**209.9**	6703(7)	3.6(3)	0.27(18)
6281(10)	30(6)	6291(10)	210.7(5), 204.8(5), 109.5(5), 69.9(5)	6245(7)	**317.1**, 209.9, 204.8, 112.2, 107.1	6704(7)	24.9(17)	4.9(33)
6208(10)	18(5)			6199(7)	**361.7**, 317.1, 209.9, 204.8 151.7, 112.2, 107.1	6702(7)	17.3(12)	5.2(35)
				6192(7)	204.8, 167.6	6705(7)	0.9(1)	0.28(19)
				6167(8)	**397.9(3)**	6705(8)	0.09(2)	0.04(3)
				6088(9)	*473.4(4)*	*6700(9)*	*0.03(1)*	*0.03(2)*
				6049(9)	**526.1(4)**	6713(9)	0.03(1)	0.04(3)
				6015(8)	**553.2(3)**	6705(8)	0.05(1)	0.09(6)
				5995(8)	**570.3(3)**, *317.1*, *253(1)*, 209.9, 204.8	6702(8)	0.07(2)	0.15(11)
				5977(8)	**595.9(5)**, 391.2(3), 386.5(3), *317.1*, 279.6(3), 209.9, 204.8	6709(8)	0.16(2)	0.38(27)
				5887(8)	**677.5(7)**, 570.3(3), 472.5(4), 467.9(4), 209.9, 204.8	6699(8)	0.12(2)	0.46(36)
				5873(8)	**695.1(5)**, 491.2(4), 486.1(3), *361.7*, *333(1)*, 209.9, 204.8	6702(8)	0.10(2)	0.70(50)

[a]However, we determined multipolarities of γ-ray transitions are listed in Table II. To evaluate lower limits of the transition intensities in the cases of ambiguous or unknown multipolarities, internal conversion coefficients for specific multipolarities were chosen as described in Table II. Intensities for transitions with known multipolarities are therefore upper limits. However, we determined multipolarities for the most intense γ-ray transitions and possible shifts of α-decay intensities caused by the unknown character of remaining (mostly higher-energy) γ decays would be small. For simplicity we thus state resulting α-decay intensities as values instead of limits.
[b]The half-life value determined from the same data set in our previous β-decay study of ^{180}Tl [8].
[c]The uncertainty of γ-ray transition energies is 0.2 keV, if not stated otherwise.
[d]Proposed in our work as being due to $\alpha + e^-$ summing (see Sec. III A).

in ^{176}Au. The data were collected in the same experiment in which the β-delayed fission [7,9] and β decay [8] of ^{180}Tl were studied. The present paper concentrates on the detailed α-decay investigation of this isotope.

II. EXPERIMENT

The measurement was performed at the ISOLDE facility (Isotope Separator On Line DEvice) at CERN [14,15]. Nuclei of ^{180}Tl were produced in proton-induced spallation reactions in a 50 g/cm^2 thick UC_x target. The beam of 1.4 GeV protons with an intensity up to 2.1 μA was supplied by the Proton-Synchrotron Booster (PSB). The nuclei produced diffused through the target heated to $\approx$2300 K and effused via the heated transfer line into a hot cavity, where Tl isotopes were selectively ionized to a charge state of 1^+ by the Resonance Ionization Laser Ion Source (RILIS) [16]. Subsequently, the ions were extracted and accelerated to 30 keV by extraction electrodes and mass separated by the High Resolution Separator (HRS). By Z-selective ionization and separation according to mass-to-charge ratio, a pure beam of ^{180}Tl nuclei was obtained.

To detect decays of ^{180}Tl, the Windmill detection system was employed [7,19]. The beam was implanted into one of ten thin carbon foils (20 μg/cm^2) mounted on a rotatable wheel. At the implantation position, two silicon detectors of 300 μm thickness were placed in close geometry around the foil to detect α particles, fission fragments, and electrons. The annular detector mounted in front of the foil had a circular hole of 6 mm diameter to let the beam through to reach the foil. The active area of the annular detector was 450 mm^2, while the active area of the circular detector placed behind the foil was 300 mm^2. The total detection efficiency for α particles was $\approx$51%.

The PSB supplied protons in 2.4 μs long pulses with a 1.2 s period. Pulses were grouped into the so-called supercycle, which typically consisted of 21 pulses during this measurement. Our experiment received from 4 to 10 pulses per supercycle. At the end of each supercycle (25.2 s), the wheel with foils was rotated so that a "fresh" foil was moved to the implantation position and remaining longer-lived daughter products were removed.

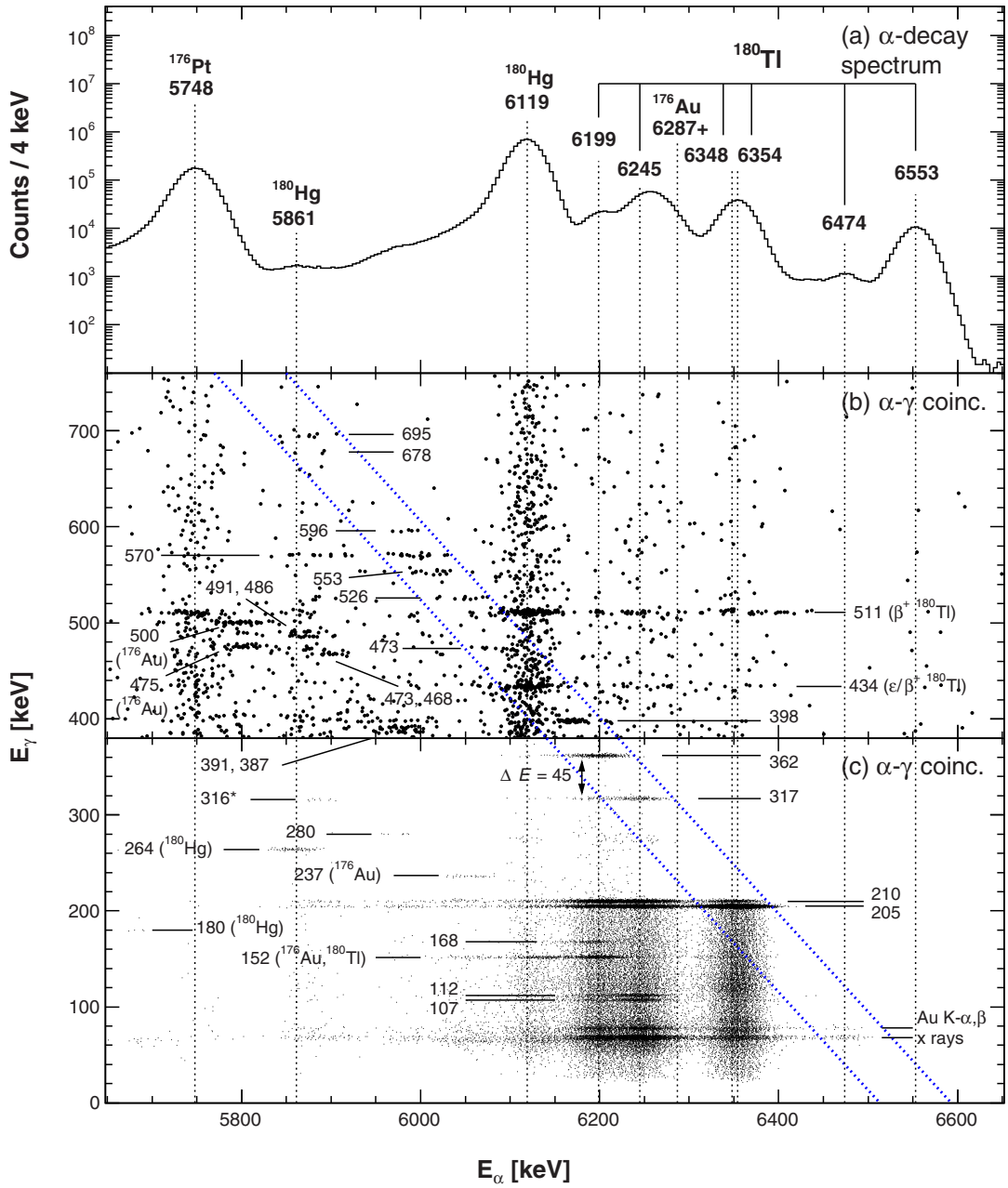

FIG. 1. (a) All α decays registered in both silicon detectors at the implantation position. The strongest α decay of the low-spin state in ^{176}Au at 6287(7) keV, marked with a plus sign, is taken from [17]. (b) α-γ coincidences for γ-ray energies in the range of 380–760 keV. (c) α-γ coincidences for γ-ray energies of 0–380 keV. For better presentation in (c), a smaller size of points was used and their density was decreased (5×). Dotted blue diagonal lines enclose α-γ groups yielding the same total $Q_{\alpha,\mathrm{tot}} = 6702(7)$ keV as the 6553-keV α decay; see the main text. The dotted lines mark the region of $Q_{\alpha,\mathrm{tot}} \pm 40$ keV. In (b) and (c), the labeled γ-ray transitions originate after α decays of ^{180}Tl if not specified otherwise. The α-γ coincidences from ^{180}Hg and ^{176}Au (except for the 475-keV transition) were assigned based on published data [17,18]. The transition marked with an asterisk is unassigned.

For the energy calibration of silicon detectors, the highest-energy α-decay transitions in ^{180}Hg, ^{180}Tl, and ^{176}Pt were the most suitable. However, the literature values for ^{176}Pt vary from $E_\alpha = 5741(8)$ keV to $E_\alpha = 5756(5)$ keV [18] and values for ^{180}Tl have uncertainties of 10 keV [12,13]. Therefore, we first performed a calibration of the detectors with the data from a run at mass number $A = 178$ with α decays of ^{178}Hg, $E_\alpha = 6429(4)$ keV [20] and ^{174}Pt, $E_\alpha = 6039(3)$ keV [18]. Based on this calibration, we deduced energies for ^{176}Pt, $E_\alpha = 5748(7)$ keV and the highest-energy α decay of ^{180}Tl, $E_\alpha = 6553(7)$ keV in the $A = 180$ run, which followed shortly after the run with $A = 178$. Consistency of the calibration for the $A = 180$ run was tested on ^{180}Hg, whereby our deduced value $E_\alpha = 6119(7)$ keV was in agreement with the tabulated value of $E_\alpha = 6119(4)$ keV from [20]. The whole data set for $A = 180$ was then calibrated using our values for ^{176}Pt and

^{180}Tl along with the known value for ^{180}Hg. The uncertainty of high-intensity α-decay peaks is defined by the systematic uncertainty of our calibration, which was 7 keV.

To detect γ and x rays, a Miniball type germanium cluster detector consisting of three independent crystals was mounted outside the vacuum behind the implantation position. Energy and relative efficiency calibrations of the cluster detector were performed using ^{152}Eu and ^{133}Ba γ-ray sources. The relative efficiency curve was scaled by the absolute efficiency value determined from α(6354 keV)-γ(205 keV) coincidences from ^{180}Tl decay. The systematic uncertainty of γ-ray energy calibration was 0.2 keV.

III. RESULTS

The energy spectrum of all α decays registered in our measurement in the two silicon detectors at the implantation position is shown in Fig. 1(a). A remarkable feature of the spectrum is its purity, with all observed activities belonging to ^{180}Tl, its daughters (^{180}Hg, ^{176}Au) and granddaughter (^{176}Pt). All α-decay transitions previously attributed to ^{180}Tl in studies [12,13] (listed in Table I) are present in our data. We note that there is a small ($\approx$10 keV) shift in the α-decay energies between our experiment and the results from [12,13]. Most probably, this shift stems from the difference in α-decay energies used for calibration in our and previous studies. Our calibration procedure is described in detail in Sec. II, while no information on the calibration energies was provided in [12,13]. A larger shift in the case of the 6245-keV transition is discussed in Sec. III B.

The detection system provided means for the investigation of α-γ and α-γ-γ coincidences, which allowed us to deduce several new fine-structure (f.s.) α decays of ^{180}Tl. The time window used in the coincidence analysis was $\Delta t(\alpha\text{-}\gamma) =$ 400 ns. Since there is a large difference in intensity between α-decay transitions to lower-lying levels and those to higher-lying levels in ^{176}Au, for a better presentation the matrix of α-γ coincidences was divided into two panels: Figs. 1(b) and 1(c). In Fig. 1(c), a smaller size of points was used and their density was decreased 5$\times$ compared to Fig. 1(b). Several f.s. α decays followed by a single-step γ-ray transition to the state fed by the highest energy (6553-keV) decay of ^{180}Tl can be readily identified based on the same total $Q_{\alpha,\mathrm{tot}} = Q_\alpha + E_\gamma$ value. The respective α-γ coincidence groups are enclosed by the dotted blue lines drawn at $Q_{\alpha,\mathrm{tot}} \pm 40$ keV.

For a better identification of the single-step transitions, we produced a projection from the region between the dotted lines to the γ-ray axis, presented in Fig. 2. The spectrum at $E_\gamma <$ 400 keV has a number of high-intensity γ-ray peaks, e.g., at 205, 210, 317, and 362 keV. The part above 500 keV is very pure, which allows a number of low-intensity γ-ray peaks to be identified, although some of them have just a few counts. Their origin will be confirmed by the analysis in following sections. The region 400–480 keV has a somewhat higher background due to random γ-ray coincidences with the most intense α decay at 6119 keV from ^{180}Hg; see Fig. 1(a). The 434-keV γ-ray peak in the region of this background belongs to the most intense transition ($2^+ \rightarrow 0^+$ in ^{180}Hg) following ε/β^+ decay, and the 511-keV γ rays come from β^+ decay of ^{180}Tl [8]. The full γ-ray spectrum from the same data set can be found in Fig. 3 of Ref. [8], which was dedicated to the β-decay study of ^{180}Tl.

Based on Fig. 2 we established excited states at 205, 210, 317, 362, 398, 473, 526, 553, 570, 596, 678, and 695 keV in ^{176}Au; see the proposed decay scheme in Fig. 3. The decay scheme was further developed based on γ-ray energy and intensity balance, determination of multipolarities for a number of transitions, and α-γ-γ coincidence analysis (see following text). Deduced energies of the ^{180}Tl f.s. α transitions and populated levels in ^{176}Au are listed in Table I alongside $Q_{\alpha,\mathrm{tot}}$ values. For γ decays in cascades in our decay scheme we investigated a possibility of energy summing in the same Ge detector, which would create artificial crossover transitions. This effect was found to be negligible. Relative γ-ray and

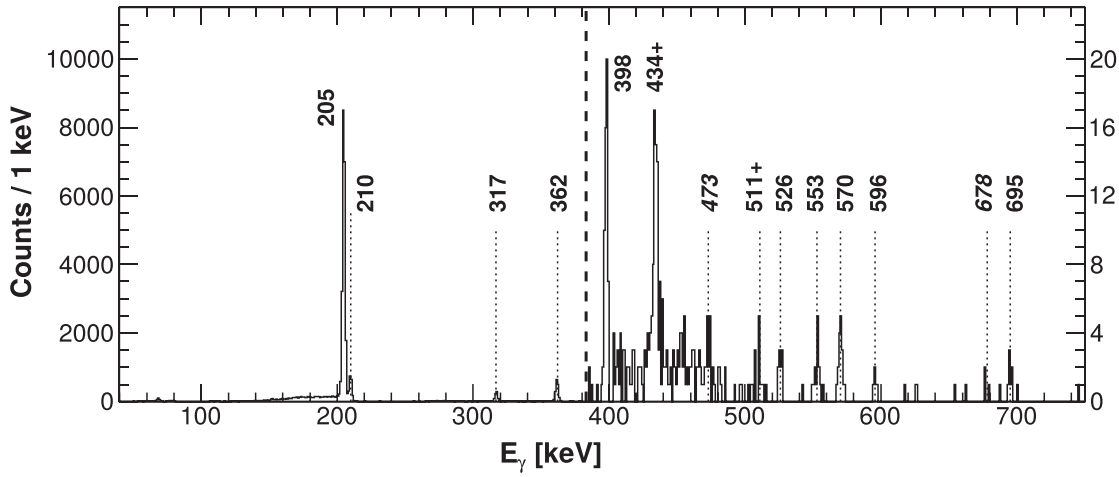

FIG. 2. γ rays in coincidence with α decays along the line of $Q_{\alpha,\mathrm{tot}}$ of the 6553-keV α decay $\pm$40 keV (a projection to γ-ray axis from the area between diagonal lines in Fig. 1). For better presentation, a different scale (1:500) is used for counts above energy of 380 keV. Tentative transitions have labels in italics, while background γ-ray peaks are marked by a plus sign.

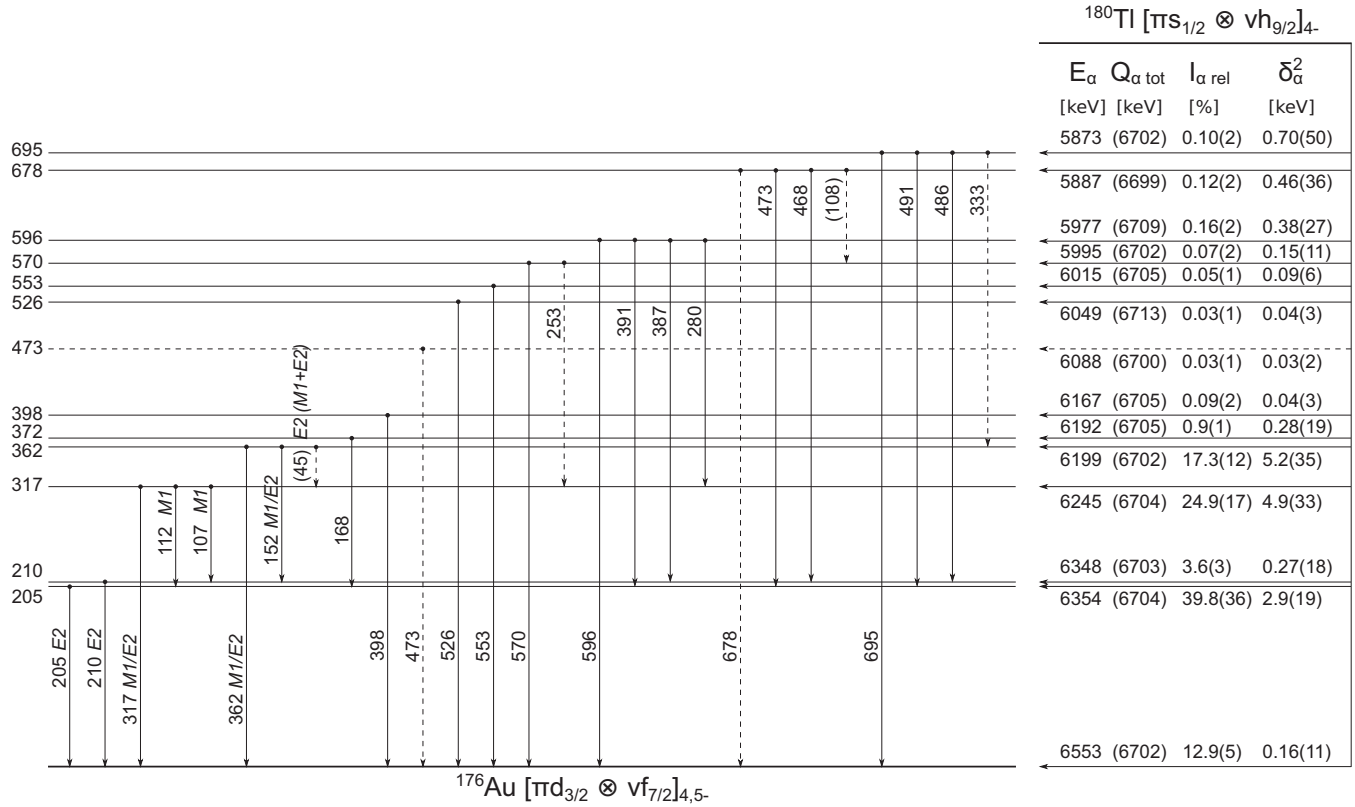

FIG. 3. Proposed α-decay scheme of ^{180}Tl. Tentative levels and transitions are denoted by dashed lines. Transitions with energies in brackets were not observed, but they were placed into decay scheme based on indirect evidence; see text for details. Labels $M1/E2$ denote the possibility of $M1$, $E2$, or mixed multipolarity. The configuration of the ground state in ^{180}Tl is taken from [21]. The tentative configuration of the daughter state in ^{176}Au is taken from [22] and is discussed in Sec. IV.

transition intensities deduced from α-γ coincidence data and multipolarities for the most intense γ decays following the α decay of ^{180}Tl are given in Table II.

A. The 205- and 210-keV levels in ^{176}Au

The 205-keV and 210-keV levels in ^{176}Au were established based on the observation of α(6354(7) keV)-γ(205 keV) and α(6348(7) keV)-γ(210 keV) coincident α-γ pairs. The 205-keV level is in agreement with the previous α-decay study [13] and both the 205- and 210-keV levels were suggested in an in-beam measurement [23].

Internal conversion of the 205-keV transition (discussed below) results in emission of K-shell conversion electrons (CE) with $E_{CE} = 124$ keV in coincidence with the feeding 6354-keV α decay. If both the CE and α particle are registered in the same silicon detector, an α+CE summing peak at $\approx$ 6478 keV is created. Therefore, we propose that the peak with $E = 6474(7)$ keV present in α-decay spectrum [Fig. 1(a)] is the result of α+CE summing. The conclusion is supported also by coincidences of the 6474-keV peak with Au K-x rays [see Fig. 1(c)]. Most probably, this summing peak corresponds to the 6470(20)/6490(10)-keV transition reported in the previous studies [12,13]. In those experiments, nuclei of ^{180}Tl were directly implanted into a silicon detector, which significantly enhances the probability of α+CE summing. Based on the discussion above, we also rule out the existence of the 64-keV level, which was suggested to be fed by the 6490-keV decay in [13].

Figure 4 shows γ rays in coincidence with the 6354- and 6348-keV α decays. The α-energy gate of 6310 keV to 6530 keV was used to cover also the region of α-CE summing events. Due to the prompt character of the 205- and 210-keV γ decays, we limit their possible multipolarities to $E1$, $M1$, or $E2$. We can determine limits of the K-conversion coefficient, α_K(205 keV), from the number of Au K-x rays and 205-keV γ rays in Fig. 4 (after correcting both numbers for detection efficiency), by assuming different multipolarities for the remaining possible source of K-x rays, the 210-keV decay. To obtain an upper limit of α_K(205 keV), we assume an $E1$ multipolarity for the 210-keV decay, which corresponds to the lowest α_K(210 keV) value. To obtain a lower limit, we assume that the 210-keV transition has an $M1$ multipolarity, which corresponds to the highest α_K(210 keV) value. Comparison of the limits with theoretical values in Table III shows that the 205-keV γ decay has to be of a pure $E2$ multipolarity. This means that the conversion of the 205-keV transition produces almost all observed Au K-x rays in Fig. 4, which further limits possible multipolarity of the 210-keV transition to $E1$ or $E2$. Based on the parity conservation argument, as further discussed in Sec. III B, we assign an $E2$ multipolarity to the 210-keV decay.

TABLE II. Relative γ-ray (I_γ) and transition (I_t) intensities and multipolarities for most intense γ decays following the α decay of ^{180}Tl. The whole energy range of ^{180}Tl fine-structure decays (5830–6550 keV) was used as the α gate. For γ rays marked with asterisks, only narrow α gates for specific α-γ groups were used to avoid mixing with γ rays of similar energy and to decrease the background. For ambiguous "$M1$ and/or $E2$" multipolarities, lower limits of the transition intensities were evaluated using internal conversion coefficients for $E2$ multipolarities. For γ rays with unknown multipolarity, lower limits of the transition intensities were evaluated using conversion coefficients for $E1$ multipolarities. All intensities are relative to the intensity of the 205-keV γ rays, which is taken as 100%.

E_γ (keV)	I_γ (%)	Multipolarity	I_t (%)
107	3.9(4)	$M1$	19.4(23)
112	4.3(5)	$M1$	19.3(23)
152*	5.5(6)	$M1$ and/or $E2$	$\geqslant$ 8.2(9)
168	1.7(2)		$\geqslant$ 1.4(2)
205	100	$E2$	100
210	39.9(47)	$E2$	39.1(46)
280*	0.13(3)		$\geqslant$ 0.10(2)
317*	3.2(5)	$M1$ and/or $E2$	$\geqslant$ 2.6(4)
362	7.6(12)	$M1$ and/or $E2$	$\geqslant$ 6.0(9)
398*	0.16(4)		$\geqslant$ 0.12(3)
570	0.19(5)		$\geqslant$ 0.14(4)

B. The 317-keV level

The 6245(7)-keV α decay feeding the 317-keV level is in coincidence with the 107-, 112-, 205-, 210-, and 317-keV γ rays [Fig. 5(a)]. By using an α-γ-γ coincidence analysis [Figs. 5(b) and 5(c)], we established that, as well as the direct 317-keV transition, this state also deexcites via two parallel cascades of the 107-210-keV and 112-205-keV γ rays.

Employing the α-γ-γ coincidences, we also determined K-conversion coefficients of the 107- and 112-keV transitions. The number of Au K-x rays was compared with the number of 107-keV γ rays (both corrected for detection efficiency), while gating on the α(6245 keV)-γ(210 keV) coincidence pair [Fig. 5(b)]. Similarly, in the case of the 112-keV transition,

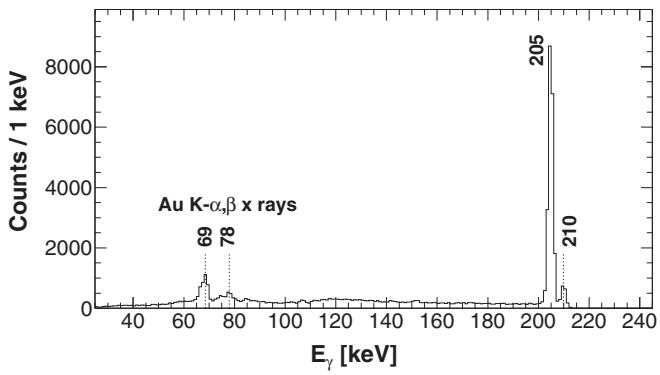

FIG. 4. γ rays in coincidence with the 6354- or 6348-keV α transitions. The α-particle energy range used for gating was 6310–6530 keV.

TABLE III. Comparison of experimental K-conversion coefficients α_K(exp) and theoretical α_K taken from [24] for possible multipolarities of listed γ decays. The α_K(205 keV) value was deduced from α-γ coincidences. The rest were determined using α-γ-γ coincidences.

E_γ (keV)	α_K(exp)	$\alpha_K(E1)$	$\alpha_K(M1)$	$\alpha_K(E2)$
205	$\leqslant$ 0.163(8) $\geqslant$ 0.105(7)	0.0556(8)	0.780(11)	0.1597(23)
107	4.3(9)	0.281(4)	4.91(7)	0.620(9)
112	3.3(6)	0.251(4)	4.30(6)	0.584(9)

we gated on the α(6245 keV)-γ(205 keV) coincidence pair [Fig. 5(c)]. The results listed in Table III show the $M1$ multipolarity as dominant for both the 107-keV and the 112-keV transitions, with a possibility of a small $E2$ admixture. Since the cascade of 112-keV($M1$)-205-keV($E2$) decays does not change parity, the 317-keV transition bypassing the cascade has to be of an $M1$ and/or $E2$ multipolarity. For the same reasons and also arguments stated in Sec. III A, the 210-keV decay from the second cascade parallel to the 317-keV decay must be of an $E2$ multipolarity.

The deduced multipolarities for the 107- and 112-keV decays can be further verified by using an alternative method as described below. Neglecting the most probably very weak transition between the 210- and 205-keV levels, subsequent γ decays in the cascades of 107-210-keV and 112-205-keV γ rays must have the same intensity (after corrections for conversion and efficiency). This characteristic allowed us to evaluate total conversion coefficients ($\alpha_{\rm tot}$) of the 107- and 112-keV decays. Results listed in Table IV confirm dominant $M1$ multipolarity for both transitions. Although $\alpha_{\rm tot}$(112 keV) is higher by 56% than the theoretical $\alpha_{\rm tot}(M1)$, $M2$ and

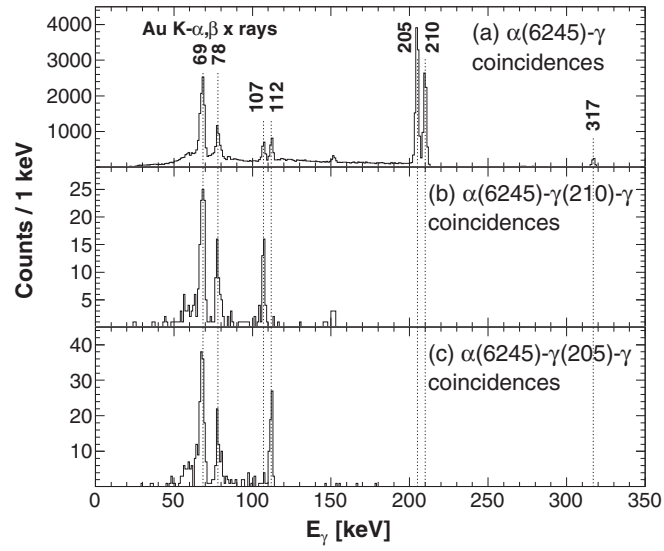

FIG. 5. γ rays in coincidence with: (a) the 6245-keV α-decay transition, (b) the 6245-keV α and 210-keV γ decay and (c) the 6245-keV α and 205-keV γ decay. The energy range used as the α gate was 6220–6320 keV.

TABLE IV. Comparison of experimental total conversion coefficients α_{tot}(exp) and theoretical α_{tot} values taken from [24] for possible multipolarities of the 107- and 112-keV γ decays.

E_γ (keV)	α_{tot}(exp)	$\alpha_{tot}(E1)$	$\alpha_{tot}(M1)$	$\alpha_{tot}(E2)$
107	5.9(6)	0.350(5)	5.98(9)	3.93(6)
112	8.2(7)	0.312(5)	5.25(8)	3.27(5)

higher multipolarities are excluded due to the prompt character of the transition. Additionally, their theoretical conversion coefficients are several times higher than our experimental value: $\alpha_{tot}(M2) = 41.0(6)$, $\alpha_{tot}(E3) = 67.7(10)$ [24]. We cannot completely rule out the possibility of a small $E0$ admixture to the 112-keV decay, although the K-conversion coefficient does not support such admixture (Table III). Relative γ-ray and transition intensities of γ decays deexciting the 317-keV level are given in Table V.

Internal conversion of the 107- and 112-keV transitions leads to emission of K-shell electrons with energies of 26.3 and 31.3 keV [24], respectively. Due to α-CE summing with the feeding 6245-keV α decay, artificial summing peaks at the energies of $\approx$6271 and $\approx$6276 keV are expected. These values are close to the α-decay energy of 6281(10) keV reported in [12] or 6291(10) keV from [13]. As discussed in connection with the 6474-keV summing peak in Sec. III A, the α-CE summing should be significantly stronger in the measurements at the FMA with activity directly implanted into a silicon detector. Furthermore, both the 107- and 112-keV transitions have over 4$\times$ higher probability of decaying via K conversion than via γ-ray emission [see the theoretical $\alpha_K(M1)$ in Table IV]. Therefore we propose that the 6281(10)/6291(10)-keV activity observed in [12,13] was an artificial peak created by full-energy summing of CE with the 6245-keV decay. On these grounds, we rule out the 275-keV level proposed to be fed by the 6291-keV transition in the previous study [13]. In agreement with the nonexistence of this level, we also did not observe the 70-keV γ rays proposed in [13] to deexcite the 275-keV level. We note that based on α-decay energies of 6281(10) and 6208(10) keV from [12] and observation of the 283- and 360-keV γ rays in the in-beam spectrum of ^{176}Au, the levels at 283- and 360-keV were proposed in [23] to be fed by these α decays. However, we did not find evidence for either of these states populated by α decays of ^{180}Tl and did not observe the 283- or 360-keV γ rays. Since there is no shift in γ-ray energy calibration (as can be seen for example for the 205- and 210-keV γ rays) between our measurement and the in-beam study [23], we rule out a possibility that the previously proposed 360-keV level is the same state as the 362-keV level discussed in Sec. III C.

TABLE V. Relative γ-ray and transition intensities of decays deexciting the 317- and 362-keV levels. Internal conversion coefficients for $E2$ multipolarities were used to evaluate transition intensities for decays with multipolarity "$M1$ and/or $E2$."

317-keV level			
E_γ (keV)	I_γ (%)	Multipolarity	I_t (%)
107	34(3)	$M1$	46(5)
112	40(3)	$M1$	48(5)
317	26(3)	$M1$ and/or $E2$	5.8(8)
362-keV level			
E_γ (keV)	I_γ (%)	Multipolarity	I_t (%)
(45)[a]	16(1)	$M1 + E2$ or $E2$	40(3)
152	37(4)	$M1$ and/or $E2$	36(3)
362	46(7)	$M1$ and/or $E2$	24(3)

[a]γ decay was not observed directly; γ-ray and transition intensities were evaluated based on the 317-, 112-, and 107-keV γ rays in coincidence with the 6199-keV α decay.

C. The 362-keV level

In addition to a direct 362-keV γ ray to the state fed by the 6553-keV α decay, the 6199(7)-keV α decay is in coincidence with the 107-, 112-, 152-, 205-, 210-, and 317-keV γ rays [Fig. 6(a)]. Gating on the respective 107-, 112-, 205-, 210-, and 317-keV γ peaks confirmed that these γ rays are indeed in coincidence with the 6199-keV α decay and do not come only from overlapping of the α-energy gate with the 6245-keV decay. Thus there has to be a 45-keV transition between the 362- and 317-keV states, which was not observed, presumably due to its high conversion. From the level of the background around the energy of 45-keV and the number of the 107-, 112-, and 317-keV γ rays in coincidence with the 6199-keV α decay, we deduced a limit of total conversion coefficient for the 45-keV decay, $\alpha_{tot} \geqslant 50$. The value is between theoretical values $\alpha_{tot}(M1) = 13.43$ and $\alpha_{tot}(E2) = 210.1$ [24], which means the 45-keV transition has a mixture of $M1 + E2$ or a pure $E2$ multipolarity. We can rule out higher multipolarities, since this transition competes with the prompt parallel 362-keV decay. As the $M1$ and $E2$ multipolarities and the subsequent 317-keV decay do not change parity, the 362-keV decay has to be of $M1$ and/or $E2$ multipolarity. The 152- and 210-keV transitions form a cascade parallel to the 362-keV decay (Fig. 3), which is shown by α-γ-γ coincidences [Fig. 6(b)]. For the same reasons as for the 362-keV decay, the 152-keV transition cannot change parity and possible multipolarities are $M1$ and/or $E2$. Relative γ-ray and transition intensities of γ decays deexciting the 362-keV level are listed in Table V.

D. The 372-keV level

While gating on the α-energy region around the 6199-keV transition, we observed 168-keV γ rays in coincidence with the 205-keV γ decay [Fig. 6(c)]. The sum of these two γ-ray transitions gives the energy of 372.4(3) keV, therefore this cascade cannot originate from deexcitation of the 362-keV level. A 372 keV level was thus established. We did not observe any clear α-γ coincidences involving the 372-keV γ-ray transition, so to determine the energy (and also intensity in Table I) of α decay feeding the 372-keV level, we gated on the 168-keV γ rays. The resulting α-transition energy was 6192(7) keV.

E. Higher-lying levels

The available statistics for α-γ coincidences, which established levels above the 372-keV state in Fig. 3, ranged

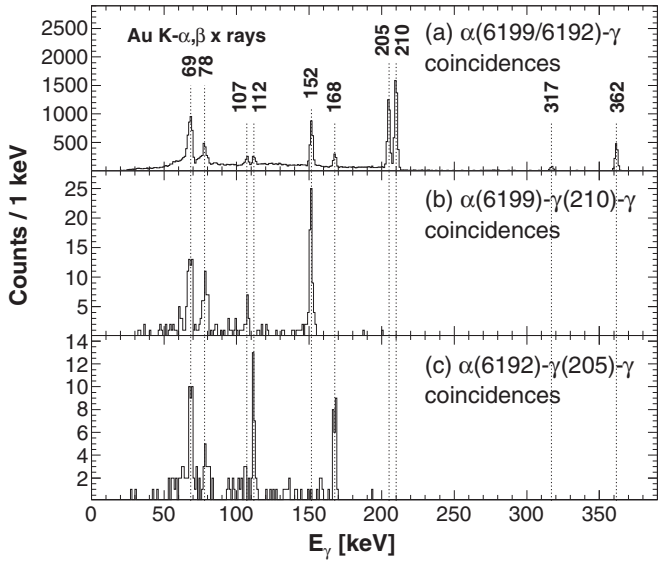

FIG. 6. γ rays in coincidence with (a) the 6199-keV or 6192-keV α-decay transition, (b) the 6199-keV α and 210-keV γ decay, and (c) the 6192-keV α and 205-keV γ decay. The energy range used as the α gate was 6150–6210 keV.

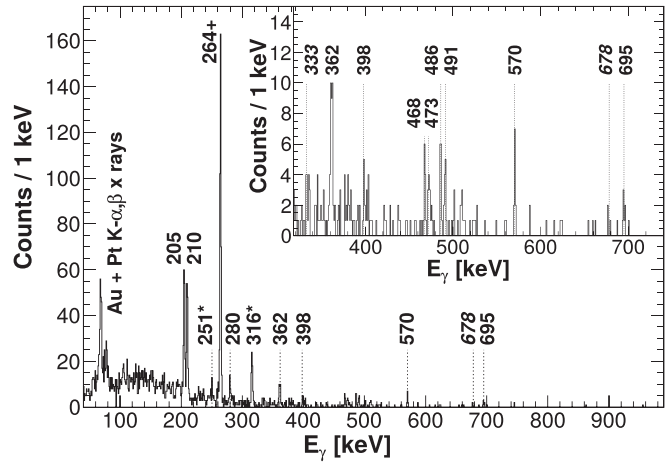

FIG. 8. γ rays in coincidence with α decays in the region of 5830–5910 keV. The inset shows an expanded part of the spectrum for the energy region of 320–740 keV. Transitions marked by asterisks are unassigned. The 264-keV γ rays marked by the plus sign originate from the α decay of ^{180}Hg. The remaining γ ray peaks are assigned as coincident with 5873- or 5887-keV α decays of ^{180}Tl. The labels in italics denote tentative assignments.

from a few counts up to a few dozens of counts [Figs. 1(b) and 2]. We could not draw any conclusions on the multipolarity of γ decays discussed in this section, except for the limitation to $E1$, $M1$, $E2$, or $M2$ due to their prompt character. We stress, that Au $K-\alpha,\beta$ x rays and the 205-, 210-keV γ rays are quite strongly present in coincidences with α decays in energy region of 5850–6100 keV [Fig. 1(c)]. These coincidences mean that there have to be several f.s. α decays in this energy region feeding the higher-lying levels. These levels then deexcite via γ-ray cascades through lower-lying (e.g., 205-, 210-keV) states and/or via single-step transitions, which is further corroborated by our data, as shown below.

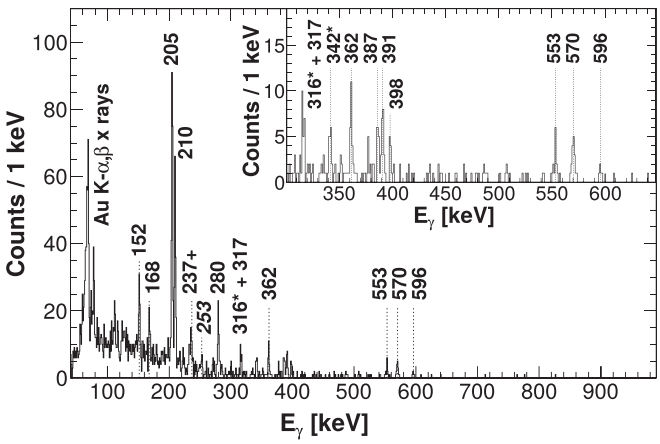

FIG. 7. γ rays in coincidence with α decays in the region of 5944–6035 keV. The inset shows an expanded part of the spectrum for the energy region of 300–650 keV. The transition marked with the plus sign originates from the α decay of ^{176}Au; transitions marked by asterisks are unassigned. Remaining γ-ray peaks are assigned as coincident to 5977- or 5995-keV α decays of ^{180}Tl. The label in italics denotes tentative assignment.

The α decay feeding the 596-keV level is, within statistical uncertainty, in coincidence with the 596-, 391-, 387-, 280-, 210-, and 205-keV γ rays and weakly also with the 317-keV γ rays [Figs. 1(b), 1(c), and 7]. Based on energy sums, we propose that, as well as by the 596-keV γ decay, the level deexcites via parallel cascades of the 391-205-, 387-210-, and 280-317-keV decays (Fig. 3). From coincidences with the 596-, 391-, 387-, and 280-keV γ rays, the energy of the α-decay transition feeding the 596-keV level was determined to be 5977(8) keV.

Using the same approach as in the previous case, we suggest additional decay paths for the 678- and 695-keV levels, which are shown in the decay scheme in Fig. 3. Parallel cascades of the 473-205-, 468-210-, and (108)-570-keV γ decays were proposed for deexcitation of the 678-keV state, while cascades of the 491-205- and 486-210-keV γ rays were suggested for decay of the 695-keV level. The 108-keV γ-ray transition between the 678- and 570-keV states was not observed, but its presence was indicated by coincidences of the 570-keV γ rays with α decays of approximately the same energy as decays in coincidence with the 678-keV γ rays. The energy of the α decay feeding the 678-keV level was then determined to be 5887(8) keV from coincidences with the 678-, 570-, 473-, and 468-keV γ-ray transitions, while the energy of the decay feeding the 695-keV state was deduced to be 5873(8) keV based on coincidences with the 695-, 491-, and 486-keV γ rays [Figs. 1(b) and 8]. Two additional connecting transitions to lower lying levels were tentatively assigned due to observation of the 253-keV γ rays in coincidence with α decays in the energy region around 5995 keV (Fig. 7) and the 333-keV γ rays in coincidence with α decays around 5873 keV (Fig. 8).

F. α decay of ^{176}Au and ^{172}Ir

In our experiment, ^{176}Au could be produced only by α decay of ^{180}Tl. Previously, the α decay of ^{176}Au was studied in [23,25–27], with the most recent and detailed investigation performed at SHIP in GSI [17]. Since two α-decaying isomers are known in ^{176}Au and it is not yet established which one is the ground state, we refer to them as "low-spin" (^{176}Au^{ls}) and "high-spin" (^{176}Au^{hs}) isomers. In our study, α-decay transitions from ^{176}Au are hidden by parent decays of ^{180}Tl in the singles α-decay energy spectrum in Fig. 1(a). The expected position of the strongest transition of the ^{176}Au^{ls} at 6287 keV is marked in the figure. However, we could clearly see the decay of ^{176}Au^{ls} via α-γ coincidences in Figs. 1(b) and 1(c), namely α-γ groups reported previously [17]: α(5798(10) keV)-γ(500 keV), α(6054(7) keV)-γ(237 keV), and α(6138(7) keV)-γ(152 keV). We did not observe any α-γ coincidences from the ^{176}Au^{hs}. Therefore we conclude that the observed α decays of ^{180}Tl populate only ^{176}Au^{ls} and a range of higher-lying levels deexciting to this state. This fact will be used in the discussion of the possible spin and configuration of ^{176}Au^{ls} (see Sec. IV).

Additionally, due to higher statistics than in the previous study [17], we identified a coincidence group of α(5806(10) keV)-γ(475 keV) in Fig. 1(b), which has an α-decay energy close to α(5798(10) keV)-γ(500 keV) coincidences from ^{176}Au^{ls}. Therefore, we tentatively suggest these two γ decays to be in coincidence with the same f.s. α decay. It would mean that there is either a 475-keV level, above the ^{172}Ir^{ls}, fed by an unobserved 25-keV transition from the 500-keV level, or a 25-keV level fed by the 475-keV transition from the 500-keV state. However, we lack additional evidence to clarify the situation.

The low-spin isomer in ^{172}Ir is populated by the α decay of ^{176}Au^{ls} [17]. It was reported to decay via a 5510(10)-keV transition to an excited state in ^{168}Re, which then deexcites by the 90-, 123-, and 136-keV γ rays [28]. Ordering of these three γ decays was not established. In our experiment, the α decay of ^{172}Ir^{ls} overlapped with the f.s. α-decay transition from ^{176}Pt with an energy of 5527(7) keV (the tabulated value is 5530(3) keV [18]), which feeds a 228-keV level in ^{172}Os [18]. However, we clearly observed coincidences of α decays around the energy of 5510 keV with the 90-, 123-, and 136-keV γ rays, confirming the presence of the ^{172}Ir^{ls}. Due to insufficient statistics for α-γ-γ coincidences, no further information on the placement of these γ decays could be obtained from our data.

G. Additional α-γ coincidences

We identified six more α-γ coincidence groups; α(5896(7) keV)-γ(316 keV) is present in Fig. 1(c), while the remaining groups are too weak to be visible in Fig. 1(c), but γ rays from them are shown in Fig. 7 and 8: α(6030(10) keV)-γ(316 keV), α(6007(8) keV)-γ(362 keV), α(5881(8) keV)-γ(362 keV), α(6000(8) keV)-γ(342 keV), α(5890(8) keV)-γ(251 keV).

The three groups with α-decay energies below 6000 keV yield $Q_{\alpha,\mathrm{tot}}$ values of 6275(8) keV and higher, which in combination with the high purity of the ion beam indicates that these coincidences come from the decay of either ^{180}Tl or ^{176}Au. The remaining α-γ groups yield $Q_{\alpha,\mathrm{tot}}$ values above 6470 keV and should originate only from decay of ^{180}Tl. Further, if we assume that the 316-keV γ rays come from the same level in both groups, and make the same assumption for the 362-keV γ rays, then all of these α-γ(316 keV) and α-γ(362 keV) groups have to originate from the decay of ^{180}Tl.

We note that the 316- and 362-keV γ rays add up to the energy of the 678-keV level. However, considering the $Q_{\alpha,\mathrm{tot}}$(^{180}Tl), the higher-energy α decay (6030 keV) in coincidence with the 316-keV transition could populate only levels up to $\approx$540 keV. Furthermore, following the decay scheme in Fig. 3 and relative intensities in Table V, the α decays in coincidence with the 316-keV transition would have to be in coincidence also with the 362- and 152-keV γ rays with intensities of $\approx$40% compared to the intensity of the 316-keV decay. Please note that the 152-keV γ rays may have even higher intensity due to possible admixture of known γ rays following α decay of ^{176}Au; see Fig. 1 and Sec. III F. Yet, only the 362-keV decay is in coincidence with the lower-energy α-decay (5896 keV) from the two α-γ(316 keV) coincidence groups, while the 152-keV γ rays are not visible above the background (Fig. 8). Hence, we did not place the 316-keV γ-ray transition into the decay scheme. The absence of the 152-keV γ rays also leads us to conclude that the 362-keV peak in Fig. 8 is a doublet formed by the transition from the 362-keV level and additional γ rays with similar energy and unknown origin. The slightly broader distribution of events in the peak supports this conclusion.

Due to similar energies of coinciding α decays, the groups containing the 362-keV γ rays may come from decay of the 678- and 553-keV levels, while the 342-keV γ rays may be in decay path of the 570-keV state. Nevertheless, we lack connecting transitions to form deexcitation cascades. Since there are several f.s. α decays of the ^{180}Tl in this energy region, we refrain from definitive placements into the decay scheme based on any of the α-γ coincidences discussed in this section.

IV. DISCUSSION

Configurations of ground states (g.s.) and low-spin isomeric states in odd-odd neutron-deficient Tl isotopes were already discussed in our previous papers dedicated to $^{178–184}$Tl [5,6,8], therefore here we briefly summarize the main features. In the heavier even-A Tl isotopes, e.g., $^{186–194}$Tl, configurations $[\pi 3s_{1/2} \otimes \nu 1i_{13/2}]_{7^+}$ and $[\pi 3s_{1/2} \otimes \nu 3p_{3/2}]_{2^-}$ and/or $[\pi 3s_{1/2} \otimes \nu 2f_{5/2}]_{2^-}$ were suggested as dominant for the ground or low-lying isomeric states [2,29–32]. Recently, 2^- and 7^+ states in ^{184}Tl ($N = 103$) and the low-spin state in ^{182}Tl ($N = 101$) were identified as well [5]. In lighter Tl isotopes with $N \leqslant 100$, a change of the neutron configuration to $\nu 1h_{9/2}$ is expected due to complete depletion of the orbitals $\nu 1i_{13/2}$ and $\nu 3p_{3/2}$ [6]. Configurations containing the $\nu 1h_{9/2}$ orbital were already proposed in other $N = 99$ isotones, e.g., for the g.s. in ^{181}Pb [33] and the low-lying excited state in ^{179}Hg [34,35]. Indeed, the β-decay study of ^{180}Tl constrained the spin and parity of the low-spin α- and β-decaying state to $4,5^-$ and the configuration of $[\pi 3s_{1/2} \otimes \nu 1h_{9/2}]_{4,5^-}$ was suggested [8]. Finally, our recent laser-spectroscopy study

supported the $[\pi 3s_{1/2} \otimes \nu 1h_{9/2}]$ configuration, $I^\pi = 4^-$ and nearly spherical shape for the g.s. of ^{180}Tl [21].

Reduced α-decay widths, δ_α^2, deduced in our study, for the five highest-energy decays of ^{180}Tl (calculated using the Rasmussen approach [36], assuming $\Delta L = 0$ transitions) are listed in Table VI. All transitions have $\delta_\alpha^2 \lesssim 5$ keV, which means they are hindered compared to unhindered decays of neighboring isotopes, e.g., ^{179g,179m}Tl with δ_α^2 values of 50(3) and 89(4) keV [37,38] or ^{183}Tl with $\delta_\alpha^2 = 41(6)$ keV [39]. When compared to the average of quoted values, the δ_α^2 value for the highest-energy transition of ^{180}Tl (6553 keV) yields a hindrance factor of ≈ 400. We already ruled out the population of a high-spin isomer in ^{176}Au (with suggested configuration of $[\pi 11/2^-(h_{11/2}) \otimes \nu 7/2^-(h_{9/2}f_{7/2})]_{8,9^+}$ [17]) based on the absence of α-γ coincidences from its decay. Further, as no isomeric α decay was observed in ^{180}Tl, this 6553-keV α transition is assigned as connecting the ^{180}Tl g.s. and ^{176}Au low-spin state. Thus, we rule out the previously suggested configuration of $[\pi 1/2^+(s_{1/2}) \otimes \nu 7/2^-(h_{9/2}f_{7/2})]_{3,4^-}$ [13,17,23] for ^{176}Au^{ls}, as it would not be in agreement with the deduced hindrance factor of ≈ 400. This earlier-suggested dominant configuration of the ^{176}Au^{ls} overlaps to a large extent with the g.s. configuration of ^{180}Tl proposed by laser-spectroscopy studies [21]. Therefore, the α decay between these two configurations would be quasi-unhindered. However, our recent laser-spectroscopy measurement and extracted magnetic moment suggest a different configuration of $[\pi d_{3/2} \otimes \nu f_{7/2}]$, $I^\pi = (4,5^-)$ and spherical shape for ^{176}Au^{ls} [22]. This configuration means that both proton and neutron have to change orbitals ($\pi s_{1/2} \rightarrow \pi d_{3/2}$ and $\nu h_{9/2} \rightarrow \nu f_{7/2}$), which is likely the reason for the strongly hindered 6553-keV α decay between the states.

The ^{176}Au^{ls} then decays to the ^{172}Ir^{ls} by unhindered or only weakly hindered α decay with $\delta_\alpha^2 = 25(3)$ keV [17]. Therefore, these states are expected to have the same parity and configuration, and the same or similar value of spin.

Most of the f.s. α decays of ^{180}Tl feeding the excited states of ^{176}Au^{ls} (Table I) are strongly hindered with δ_α^2 values below 1 keV; some of them are even below 0.1 keV. This fact indicates that also states populated by these decays have significantly different configurations compared to the g.s. of ^{180}Tl. The 6354-, 6245-, and 6199-keV decays are exceptions with δ_α^2 values of a few keV, which suggest that states fed by these decays have more similar structure to the g.s. of ^{180}Tl than other levels above ^{176}Au^{ls} identified in this work (e.g., there may be a change of only the proton or neutron configuration). We note that there is a similar pattern in ^{178}Tl, where the full-energy decay [6862(10) keV] to the low-spin isomer in ^{174}Au is strongly hindered, while the decays to the 173- and 273-keV states above ^{174}Au^{ls} are hindered only moderately with $\delta_\alpha^2 \approx 10$ keV [6]. Although we determined multipolarities for some of the γ-ray transitions following f.s. α decays of ^{180}Tl, we refrain from detailed discussion of I^π and configurations for states above the α-decaying ^{176}Au^{ls} since the exact spin of this state is not yet established and various competing configurations may arise from coupling of unpaired proton and neutron in this nucleus.

Systematics of δ_α^2 values for α decays of low-spin states in odd-odd thallium isotopes ^{178,180,182,184}Tl are shown in Table VI. All decays are hindered, although two decays of ^{178}Tl are hindered only moderately. Overall, transitions in these isotopes (see also Table I for all decays of ^{180}Tl) can be divided into three groups according to their δ_α^2 values. Decays in the first group have δ_α^2 of a few keV (with the exception of ^{178}Tl with values around 10 keV), values in the second group are from the range of $0.1 < \delta_\alpha^2 < 1$ keV, and in the third group δ_α^2 are smaller than 0.1 keV. The highest-energy α decay for each isotope is strongly hindered, with values of $\delta_\alpha^2 < 0.6$ keV, which emphasizes that in all four cases the structures of the parent and daughter states are significantly different. However, only a detailed study of the ground-state properties of the even-A Au isotopes would allow the reasons behind this general trend to be revealed.

TABLE VI. α-decay energies and reduced widths of α decays for ^{180}Tl and low-spin states in neighboring odd-odd Tl isotopes. Only the five highest-energy decays are shown for ^{180}Tl.

^{178}Tl [6]		^{180}Tl (This work)	
E_α (keV)	δ_α^2 (keV)	E_α (keV)	δ_α^2 (keV)
6862(10)	0.30(15)	6553(7)	0.16(11)
6693(10)	13.0(17)	6354(7)	2.9(19)
6595(10)	10.2(24)	6348(7)	0.27(18)
		6245(7)	4.9(33)
		6199(7)	5.2(35)
^{182}Tl [5]		^{184}Tl [5]	
E_α (keV)	δ_α^2 (keV)	E_α (keV)	δ_α^2 (keV)
6406	> 0.017	6161	0.57(6)
6360(6)	> 0.019	5988(12)	2.4(4)[a]
6165(6)	> 0.45	5964(12)	
6046(5)	> 2.3	5810(12)	0.9(1)
5962(5)	> 2.4	5748(12)	< 0.09

[a]A common value for both the 5988- and 5964-keV α decays was stated. The dominant contribution was from the 5988-keV decay.

V. CONCLUSIONS

A detailed α-decay study of ^{180}Tl was performed employing α-γ coincidence measurements. Several new fine-structure α decays leading to excited states in the daughter-nuclide ^{176}Au were identified. Multipolarities of a few γ transitions deexciting levels in ^{176}Au were determined, which allowed a more extended decay scheme of ^{180}Tl to be established. Reduced widths of α decays were evaluated and compared with values from neighboring even-A isotopes. A strong hindrance factor of ≈ 400 for the α-decay transition connecting the ground state in ^{180}Tl and the low-spin state in ^{176}Au was observed. The hindrance was explained by significant change in configuration between the initial and final state. A similar trend of hindered α decays was previously identified also in ^{182,184}Tl [5]. Combined knowledge from α-decay studies of Tl isotopes and upcoming laser-spectroscopy studies (charge radii, magnetic moments, spins, etc.) of Au isotopes may give rise to a global description of Tl to Au α decays.

ACKNOWLEDGMENTS

We thank the ISOLDE Collaboration for providing excellent beams and the GSI Target Group for manufacturing the carbon foils. This work has been supported by FWO-Vlaanderen (Belgium), by GOA/2010/010 (BOF KU Leuven), by the Interuniversity Attraction Poles Programme initiated by the Belgian Science Policy Office (BriX network P7/12), by the European Commission within the Seventh Framework Programme through I3-ENSAR (Contract No. RII3-CT-2010-262010), by a grant from the European Research Council (ERC-2011-AdG-291561-HELIOS), by the European Union's Horizon 2020 research and innovation programme under Grant Agreement No. 654002 (ENSAR2), by the U.K. Science and Technology Facilities Council, by the Slovak Research and Development Agency (Contracts No. APVV-0105-10, No. APVV-14-0524, and No. APVV-0177-11), and by Slovak grant agency VEGA (Contracts No. 1/0532/17 and No. 2/0129/17).

[1] A. N. Andreyev *et al.*, Eur. Phys. J. A **18**, 55 (2003).
[2] P. Van Duppen *et al.*, Nucl. Phys. A **529**, 268 (1991).
[3] M. Huyse *et al.*, Phys. Lett. B **201**, 293 (1988).
[4] J. Van Maldeghem and K. Heyde, Fizika **22**, 233 (1990).
[5] C. Van Beveren *et al.*, J. Phys. G: Nucl. Part. Phys. **43**, 025102 (2016).
[6] V. Liberati, A. N. Andreyev, S. Antalic, A. Barzakh, T. E. Cocolios, J. Elseviers, D. Fedorov, V. N. Fedosseev, M. Huyse, D. T. Joss, Z. Kalaninová, U. Köster, J. F. W. Lane, B. Marsh, D. Mengoni, P. Molkanov, K. Nishio, R. D. Page, N. Patronis, D. Pauwels, D. Radulov, M. Seliverstov, M. Sjödin, I. Tsekhanovich, P. Van den Bergh, P. Van Duppen, M. Venhart, and M. Veselský, Phys. Rev. C **88**, 044322 (2013).
[7] A. N. Andreyev, J. Elseviers, M. Huyse, P. Van Duppen, S. Antalic, A. Barzakh, N. Bree, T. E. Cocolios, V. F. Comas, J. Diriken, D. Fedorov, V. Fedosseev, S. Franchoo, J. A. Heredia, O. Ivanov, U. Köster, B. A. Marsh, K. Nishio, R. D. Page, N. Patronis, M. Seliverstov, I. Tsekhanovich, P. Van den Bergh, J. Van De Walle, M. Venhart, S. Vermote, M. Veselský, C. Wagemans, T. Ichikawa, A. Iwamoto, P. Möller, and A. J. Sierk, Phys. Rev. Lett. **105**, 252502 (2010).
[8] J. Elseviers *et al.*, Phys. Rev. C **84**, 034307 (2011).
[9] J. Elseviers *et al.*, Phys. Rev. C **88**, 044321 (2013).
[10] E. Rapisarda *et al.*, J. Phys. G: Nucl. Part. Phys. **44**, 074001 (2017).
[11] C. Van Beveren, A. N. Andreyev, A. E. Barzakh, T. E. Cocolios, D. Fedorov, V. N. Fedosseev, R. Ferrer, M. Huyse, U. Köster, J. Lane, V. Liberati, K. M. Lynch, B. A. Marsh, T. J. Procter, D. Radulov, E. Rapisarda, K. Sandhu, M. D. Seliverstov, P. Van Duppen, M. Venhart, and M. Veselsky, Phys. Rev. C **92**, 014325 (2015).
[12] K. S. Toth, X.-J. Xu, C. R. Bingham, J. C. Batchelder, L. F. Conticchio, W. B. Walters, L. T. Brown, C. N. Davids, R. J. Irvine, D. Seweryniak, J. Wauters, and E. F. Zganjar, Phys. Rev. C **58**, 1310 (1998).
[13] F. G. Kondev *et al.*, EPJ Web Conf. **63**, 01013 (2013).
[14] M. J. G. Borge and B. Jonson, J. Phys. G: Nucl. Part. Phys. **44**, 044011 (2017).
[15] E. Kugler, Hyperfine Interact. **129**, 23 (2000).
[16] V. N. Fedoseyev *et al.*, Hyperfine Interact. **127**, 409 (2000).
[17] A. N. Andreyev, S. Antalic, D. Ackermann, T. E. Cocolios, J. Elseviers, S. Franchoo, S. Heinz, F. P. Heßberger, S. Hofmann, M. Huyse, J. Khuyagbaatar, B. Kindler, B. Lommel, R. Mann, R. D. Page, P. Van Duppen, and M. Venhart, Phys. Rev. C **90**, 044312 (2014).
[18] ENSDF, Evaluated Nuclear Structure Data File, http://www.nndc.bnl.gov/ensdf.
[19] M. D. Seliverstov, T. E. Cocolios, W. Dexters, A. N. Andreyev, S. Antalic, A. E. Barzakh, B. Bastin, J. Büscher, I. G. Darby, D. V. Fedorov, V. N. Fedosseev, K. T. Flanagan, S. Franchoo, G. Huber, M. Huyse, M. Keupers, U. Köster, Y. Kudryavtsev, B. A. Marsh, P. L. Molkanov, R. D. Page, A. M. Sjödin, I. Stefan, P. Van Duppen, M. Venhart, and S. G. Zemlyanoy, Phys. Rev. C **89**, 034323 (2014).
[20] F. G. Kondev *et al.*, Phys. Rev. C **62**, 044305 (2000).
[21] A. E. Barzakh *et al.*, Phys. Rev. C **95**, 014324 (2017).
[22] A. E. Barzakh (private communication).
[23] J. T. M. Goon, Ph.D. thesis, University of Tennessee, Knoxville, 2004 (unpublished).
[24] T. Kibédi *et al.*, Nucl. Instrum. Methods A **589**, 202 (2008), http://bricc.anu.edu.au/.
[25] C. Cabot *et al.*, Nucl. Phys. A **241**, 341 (1975).
[26] J. Schneider, Ph.D. thesis, Johannes-Gutenberg Universität Mainz, GSI report GSI-84-3, 1984 (unpublished).
[27] M. W. Rowe *et al.*, Phys. Rev. C **65**, 054310 (2002).
[28] W. D. Schmidt-Ott *et al.*, Nucl. Phys. A **545**, 646 (1992).
[29] A. J. Kreiner, C. Baktash, G. Garcia Bermudez, and M. A. J. Mariscotti, Phys. Rev. Lett. **47**, 1709 (1981).
[30] R. Menges *et al.*, Z. Phys. A **341**, 475 (1992).
[31] C. Ekström, G. Wannberg, and Y. S. Shishodia, Hyperfine Interact. **1**, 437 (1975).
[32] C. Bengtsson *et al.*, Phys. Scr. **30**, 164 (1984).
[33] A. N. Andreyev *et al.*, Phys. Rev. C **80**, 054322 (2009).
[34] F. G. Kondev *et al.*, Phys. Lett. B **528**, 221 (2002).
[35] D. G. Jenkins *et al.*, Phys. Rev. C **66**, 011301(R) (2002).
[36] J. O. Rasmussen, Phys. Rev. **113**, 1593 (1959).
[37] A. N. Andreyev *et al.*, Phys. Rev. C **87**, 054311 (2013).
[38] A. N. Andreyev *et al.*, J. Phys. G: Nucl. Part. Phys. **37**, 035102 (2010).
[39] P. M. Raddon *et al.*, Phys. Rev. C **70**, 064308 (2004).